

1 **Siberian tree-ring and stable isotope proxies as indicators of temperature and moisture**  
2 **changes after major stratospheric volcanic eruptions**

3

4 Olga V. Churakova<sup>1,2\*</sup>, Marina V. Fonti<sup>2</sup>, Matthias Saurer<sup>3,4</sup>, Sébastien Guillet<sup>1</sup>, Christophe  
5 Corona<sup>5</sup>, Patrick Fonti<sup>3</sup>, Vladimir S. Myglan<sup>6</sup>, Alexander V. Kirilyanov<sup>2,7,8</sup>, Oksana V.  
6 Naumova<sup>6</sup>, Dmitriy V. Ovchinnikov<sup>7</sup>, Alexander Shashkin<sup>2,7</sup>, Irina Panyushkina<sup>9</sup>, Ulf  
7 Büntgen<sup>3,8</sup>, Malcolm K. Hughes<sup>9</sup>, Eugene A. Vaganov<sup>2,7,10</sup>, Rolf T.W. Siegwolf<sup>3,4</sup>, Markus  
8 Stoffel<sup>1,11,12</sup>

9 *<sup>1</sup>Institute for Environmental Sciences, University of Geneva, CH-1205 Geneva, Switzerland*

10 *<sup>2</sup>Institute of Ecology and Geography, Siberian Federal University RU-660049 Krasnoyarsk,*  
11 *Svobodniy pr 79/10, Russia*

12 *<sup>3</sup>Swiss Federal Institute for Forest, Snow and Landscape Research WSL, Zürcherstrasse 111,*  
13 *CH-8903 Birmensdorf, Switzerland*

14 *<sup>4</sup>Paul Scherrer Institute, CH- 5232 Villigen - PSI, Switzerland*

15 *<sup>5</sup>Université Blaise Pascal, Geolab, UMR 6042 CNRS, 4 rue Ledru, F-63057 Clermont-Fer-*  
16 *rand, France*

17 *<sup>6</sup>Institute of Humanities, Siberian Federal University RU-660049 Krasnoyarsk, Svobodniy pr*  
18 *82, Russia*

19 *<sup>7</sup>Sukachev Institute of Forest SB RAS, Federal Research Center “Krasnoyarsk Science Cen-*  
20 *ter SB RAS” RU-660036 Krasnoyarsk, Akademgorodok 50, bld. 28, Russia*

21 *<sup>8</sup>Department of Geography, University of Cambridge, Downing Place, Cambridge CB2 3EN*

22 *<sup>9</sup>Laboratory of Tree-Ring Research, University of Arizona, 1215 E. Lowell St., Tucson, 85721,*  
23 *USA*

24 *<sup>10</sup>Siberian Federal University, Rectorate, RU-660049 Krasnoyarsk, Svobodniy pr 79/10, Rus-*  
25 *sia*

26 <sup>11</sup>*dendrolab.ch, Department of Earth Sciences, University of Geneva, 13 rue des Maraîchers,*  
27 *CH-1205 Geneva, Switzerland*

28 <sup>12</sup>*Department F.A. Forel for Aquatic and Environmental Sciences, University of Geneva, 66*  
29 *Boulevard Carl-Vogt, CH-1205 Geneva, Switzerland*

30

31 **Corresponding author:** Olga V. Churakova\*

32 E-Mail: [olga.churakova@hotmail.com](mailto:olga.churakova@hotmail.com)

33

34

35

36

37

38

39

40

41

42

43

44

45

46 **Abstract**

47 Stratospheric volcanic eruptions have far-reaching impacts on global climate and society. Tree  
48 rings can provide valuable climatic information on these impacts across different spatial and  
49 temporal scales. Here we explore the suitability of tree-ring width (TRW), maximum latewood  
50 density (MXD), cell wall thickness (CWT), and  $\delta^{13}\text{C}$  and  $\delta^{18}\text{O}$  in tree-ring cellulose for the  
51 detection of climatic changes in northeastern Yakutia (YAK), eastern Taimyr (TAY) and Rus-  
52 sian Altai (ALT) sites caused by six major stratospheric volcanic eruptions (535, 540, 1257,  
53 1640, 1815 and 1991).

54 Our findings suggest that TRW, MXD, and CWT show strong summer air temperature anom-  
55 alies in 536, 541-542, and 1258-1259 at all study sites. However, they do not reveal distinct  
56 and coherent fingerprints after other eruptions. Based on  $\delta^{13}\text{C}$  data, 536 was extremely humid  
57 in YAK and TAY, whereas 541 and 542 were humid years in TAY and ALT. In contrast, the  
58 1257 eruption of Samalas likely led to at least two dry summers across all three Siberian sites.  
59 No further extreme hydro-climatic anomalies occurred at Siberian sites after the 1991 eruption.  
60 Summer sunshine duration decreased significantly in 536, 541-542, 1258-1259 in YAK, and  
61 536 in ALT. We show that trees growing at YAK responded mainly during the first year after  
62 the eruptions, whereas a two years delay occurs at TAY and ALT.

63 Since climatic responses to large volcanic eruptions are different, and thus affect ecosystem  
64 functioning and productivity differently in space and time, a combined assessment of multiple  
65 tree-ring parameters is needed to provide a more complete picture of past climate dynamics,  
66 which in turns appears fundamental to validate global climate models.

67

68 **Key words:**  $\delta^{13}\text{C}$  and  $\delta^{18}\text{O}$  in tree-ring cellulose, tree-ring width, maximum latewood den-  
69 sity, cell wall thickness, drought, temperature, precipitation, sunshine duration, vapor pres-  
70 sure deficit

## 71 **1. Introduction**

72 Major stratospheric volcanic eruptions can substantially modify the Earth's radiative balance  
73 and cool the troposphere. This is due to the massive injection of sulphate aerosols, which are  
74 able to reduce surface temperatures on timescales ranging from months to years (Robock,  
75 2000). The global cooling associated with the radiative effects of volcanic aerosols, which ab-  
76 sorb terrestrial radiation and scatter incoming solar radiation significantly, has been estimated  
77 to about 0.5°C during the two years following the Mount Pinatubo eruption in June 1991 (Han-  
78 sen et al., 1996).

79 Since trees – as living organisms – are impacted in their metabolism by environmental changes,  
80 their responses to these changes are recorded in the biomass, as it is found in tree-ring param-  
81 eters (Schweingruber, 1996). The decoding of tree-ring archives therefore is used to reconstruct  
82 past climates. A summer cooling of the Northern Hemisphere (NH) ranging from 0.6°C to  
83 1.3°C has been reported after the strongest eruptions of the past 1,500 years: CE 1257 Samalas,  
84 1452/3 Unknown, 1600 Huaynaputina, and 1815 Tambora eruptions based on tree-ring width  
85 (TRW) and maximum latewood density (MXD) reconstructions (Briffa et al., 1998; Schneider  
86 et al., 2015; Stoffel et al., 2015; Wilson et al., 2016; Esper et al., 2017; Guillet et al., 2017).

87 According to climate simulations, significant changes in the precipitation regime can also be  
88 expected after large volcanic eruptions; these include, among others, rainfall deficit in monsoon  
89 prone regions and in Southern Europe (Joseph and Zeng, 2011) as well as wetter than normal  
90 conditions in Northern Europe (Robock and Liu 1994; Gillet et al., 2004; Peng et al., 2009;  
91 Meronen et al., 2012; Iles et al., 2013; Wegmann et al., 2014). However, despite recent ad-  
92 vances in the field, the impacts of stratospheric volcanic eruptions on the hydro-climatic vari-  
93 ability at regional scales remain largely unknown. Therefore, this relevant knowledge about  
94 moisture anomalies is critically needed, especially at high-latitude sites where tree growth is  
95 mainly limited by summer temperatures.

96 As dust and aerosol particles of large volcanic eruptions affect primarily the radiation regime,  
97 three major drivers of plant growth, i.e. photosynthetic active radiation (PaR), temperature and  
98 vapor pressure deficit (VPD) will be affected by volcanic activity. This is reflected in reduced  
99 TRW as a result of reduced photosynthesis but even more so by low temperature. As cell divi-  
100 sion is also temperature dependent, its rate (tree-ring growth) will exponentially decrease with  
101 decreasing temperature below +3°C (Körner, 2015), outweighing the “low light / low-photo-  
102 synthesis” effect by far.

103 Furthermore, over the last years, some studies using mainly carbon isotopic signals ( $\delta^{13}\text{C}$ ) in  
104 tree rings showed eco-physiological responses of trees to volcanic eruptions at mid- (Bat-  
105 tipaglia et al., 2007) or high- (Gennaretti et al., 2017) latitudes. By contrast, a combination of  
106 both carbon ( $\delta^{13}\text{C}$ ) and oxygen ( $\delta^{18}\text{O}$ ) isotopes in tree rings has been employed only rarely to  
107 trace CE volcanic eruptions in high-latitude or high-altitude proxy records (Churakova (Si-  
108 dorova) et al., 2014).

109 Approaches including TRW, MXD and cell wall thickness (CWT) as well as  $\delta^{13}\text{C}$  and  $\delta^{18}\text{O}$  in  
110 tree cellulose are a promising way to disentangle hydro-climatic variability as well as winter  
111 and early spring temperatures at high-latitude and high-altitude sites (Sidorova et al., 2008,  
112 2010, 2011; Churakova (Sidorova) et al., 2014). In that sense, recent work has allowed the  
113 retrieval of high-resolution, seasonal information on water and carbon limitations on growth  
114 during spring and summer from CWT measurements (Panyushkina et al., 2003; Sidorova et  
115 al., 2011; Fonti et al., 2013; Bryukhanova et al., 2015). Depending on site conditions,  $\delta^{13}\text{C}$   
116 variations reflect light (stand density) (Loader et al., 2013), water availability (soil properties)  
117 and air humidity (proximity to open waters, i.e. rivers, lakes, swamps and orography) as these  
118 parameters have been recognized to modulate the stomatal conductance ( $g_s$ ) controlling carbon  
119 isotopic discrimination.

120 Depending on the study site, a decrease in the carbon isotope ratio can be expected after strat-  
121 ospheric volcanic eruptions due to limited photosynthetic activity and higher stomatal conduct-  
122 ance, which in turn would be the result of decreased temperatures, VPD and a reduction in light  
123 intensity. By contrast, volcanic eruptions have also been credited for an increase in photosyn-  
124 thesis as dust and aerosol particles cause an increased light scattering, compensating for the  
125 light reduction (Gu et al., 2003). A significant increase in  $\delta^{13}\text{C}$  values in tree-ring cellulose  
126 should be interpreted as an indicator of drought (stomatal closure) or high photosynthesis (Far-  
127 quhar et al., 1982).

128 In the past, very limited attention has been given to the elemental and isotopic composition of  
129 tree rings in years during which they may have been subjected to the climatic influence of  
130 powerful, but remote, and often tropical, volcanic eruptions.

131 In this study, we aim to fill this gap by investigating the response of different components of  
132 the Siberian climate system (i.e. temperature, precipitations, VPD, and sunshine duration) to  
133 the largest volcanic events of the last 1,500 years. By doing so, we seek to extend our under-  
134 standing of the effects of volcanic eruptions on climate by combining multiple climate sensitive  
135 variables measured in tree rings that were formed around the time of the largest volcanic erup-  
136 tions with a Volcanic Explosivity Index (VEI) exceeding 5. We focus our investigation on  
137 remote, two high-latitude (northeastern Yakutia), YAK and eastern Taimyr (TAY) and one  
138 high-altitude (Russian Altai, ALT) Siberian sites, where long tree-ring chronologies with high  
139 climate sensitivity exist. Therefore, we developed a dataset including five tree-ring proxies:  
140 TRW, MXD, CWT,  $\delta^{13}\text{C}$  and  $\delta^{18}\text{O}$  stable isotope chronologies derived from larch trees to (1)  
141 determine the major climatic drivers of the above mentioned proxies and to evaluate their suit-  
142 ability in terms of climate responsiveness, for each proxy separately and in combination; and  
143 (2) based on these analyses reconstruct the climatic effect of these unusually large CE volcanic  
144 eruptions (Table 1).

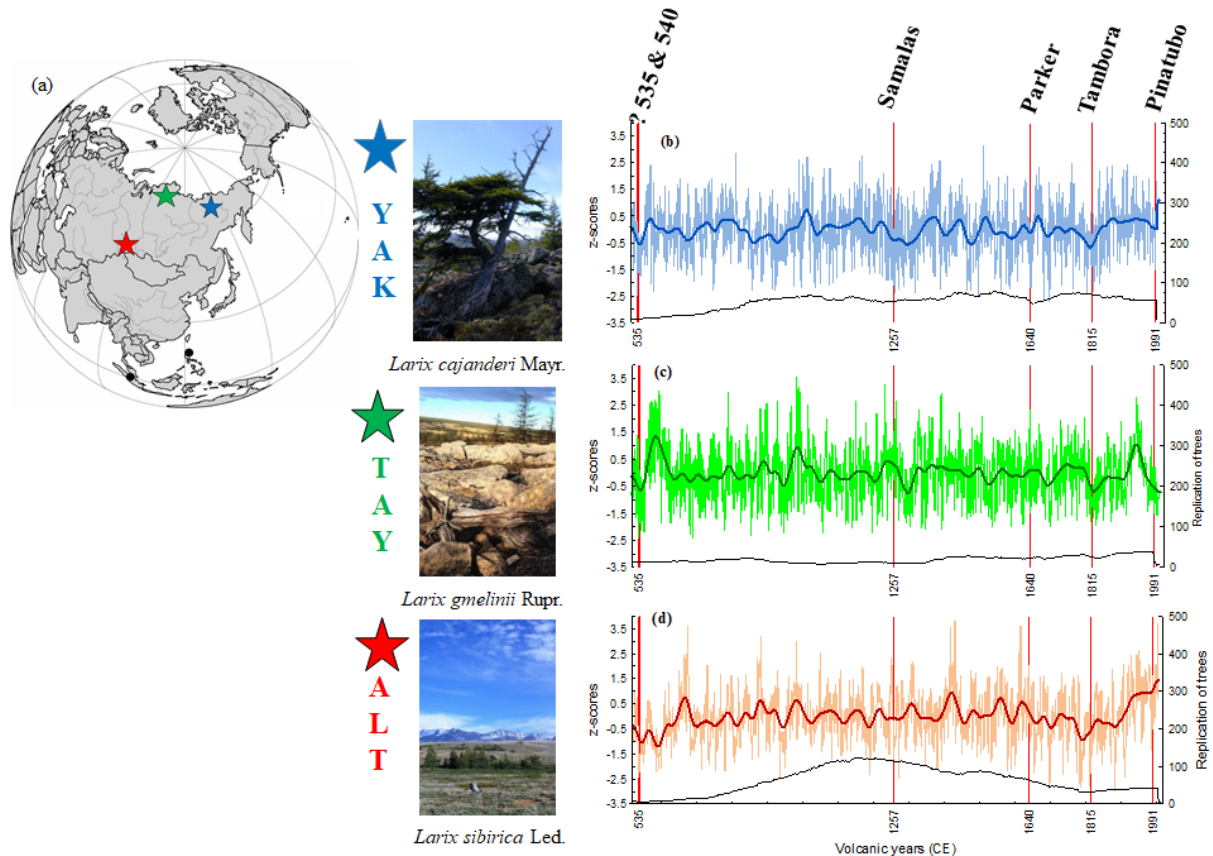
145 **2. Material and methods**

146

147 *2.1. Study sites*

148 The study sites are situated in Siberia (Russian Federation), far away from industrial centers,  
149 in zones characterized by continuous permafrost in northeastern Yakutia (YAK, 69°N, 148°E);  
150 eastern Taimyr (TAY, 70°N, 103°E) and in the Altai mountains (ALT, 50°N, 89°E) (Fig. 1a,  
151 Table 2). Tree-ring samples were collected during several expeditions and included old relict  
152 wood and living larch trees, *Larix cajanderi* Mayr (max. 1216 years) in YAK, *Larix gmelinii*  
153 Rupr. (max. 640 years) in TAY and *Larix sibirica* Ldb. (max. 950 years) in ALT. TRW chro-  
154 nologies have been developed and published in the past (Fig. 1, Hughes et al., 1999; Sidorova  
155 and Naurzbaev 2002; Sidorova 2003 for YAK; Naurzbaev et al., 2002 for TAY; Myglan et al.,  
156 2008 for ALT).

157 Mean annual air temperature is lower at the high-latitude YAK and TAY sites than at the high-  
158 altitude ALT site (Table 2). Annual precipitation totals are very low for all study sites. The  
159 vegetation period calculated with a growth threshold of +5°C (Fritts 1976; Schweingruber  
160 1996) is very short (50-120 days) at all locations (Table 2). Sunshine duration for tree growth  
161 is higher at YAK and TAY (ca. 18-20 h/day in summer) compared to ALT (ca. 18 h/day in  
162 summer) (Sidorova et al., 2005; Myglan et al., 2008; Sidorova et al., 2011; Churakova (Si-  
163 dorova) et al., 2014).



164  
 165 **Fig. 1.** Map with the locations of the study sites (stars) and volcanic eruptions from the tropics  
 166 (black dots) considered in this study (a). Annual tree-ring width index (light lines) and  
 167 smoothed by 51-year Hamming window (bold lines) chronologies from northeastern Yakutia  
 168 (YAK - blue, b) (Hughes et al., 1999; Sidorova and Naurzbaev 2002; Sidorova 2003), eastern  
 169 Taimyr (TAY - green, c) (Naurzbaev et al., 2002), and Russian Altai (ALT - red, d) (Myglan  
 170 et al., 2009) were constructed based on larch trees (Photos: V. Myglan – ALT, M. M.  
 171 Naurzbaev – YAK, TAY).

172  
 173 *2.2. Selection of the study periods and larch subsamples*

174 Volcanic aerosols deposited in ice core records (Gao et al., 2008; Crowley and Untermann,  
 175 2013; Sigl et al., 2015) attest to 6 major volcanic events in CE 535, 540, 1257, 1640, 1815, and  
 176 1991 with the VEI>6, that may have had a noticeable impact on the climate system globally.



177 To investigate climatic impacts of these eruptions in Siberian regions we developed MXD,  
178 CWT,  $\delta^{13}\text{C}$  and  $\delta^{18}\text{O}$  chronologies for the following periods around ( $\pm 10$  years): CE 525-545,  
179 1247-1267, 1630-1650, 1805-1825, and 1950-2000, with the latter being used to calibrate tree-  
180 ring proxy versus available climate data (Table 2).

181 Material was prepared from the 2000-yr long TRW chronologies available at each of the sites  
182 from the previous studies (Fig. 1 b-d). According to the level of conservation of the material,  
183 the largest possible number of samples was prepared for each of the proxies. Unlike TRW,  
184 which could be measured on virtually all samples, some of the material was not available with  
185 sufficient quality to allow for tree-ring anatomy and stable isotope analysis. We therefore use  
186 a smaller sample size for CWT (n=4) and stable isotopes (n=4) than for TRW (n=12) or MXD  
187 (n=12). Nonetheless, replications are still comparable with those used in reference papers in  
188 the fields of CWT and isotope analyses (Loader et al., 1997; Panyushkina et al., 2003; Fonti et  
189 al., 2013).

190

191

192

193 **Table 1.** List of stratospheric volcanic eruptions used in the study.

<b>Study period (CE)</b>	<b>Date of eruption Month/Day/Year</b>	<b>Volcano name</b>	<b>Volcanic Explosivity Index (VEI)</b>	<b>Location, coordinates</b>	<b>References</b>
525-545	NA/NA/535	Unknown	?	Unknown	Stothers, 1984
	NA/NA/540	Unknown	?	Unknown	Sigl et al., 2015
1247-1267	May-October/NA/ 1257	Samalas	7	Indonesia, 8.42°N, 116.47°E	Lavigne et al., 2013; Stothers, 2000; Sigl et al., 2015
1630-1650	December/26/1640	Parker	5	Philippines, 6°N, 124°E	Zielinski et al., 1994
1805-1825	April/10/1815	Tambora	7	Indonesia, 8°S, 118°E	Zielinski et al., 1994
1950 - 2000	June/15/1991	Pinatubo	6	Philippines, 15°N, 120°E	Zielinski et al., 1994; Sigl et al., 2015

194 NA – not available.

195

196

197

198

199 **Table 2.** Summary of tree-ring sites in northeastern Yakutia (YAK), eastern Taimyr (TAY), and Altai (ALT) and weather stations used in the  
 200 study. Monthly air temperature (T, °C), precipitation (P, mm), sunshine duration (S, h/month) and vapor pressure deficit (VPD, kPa) data were  
 201 used from the available meteorological database: <http://aisori.meteo.ru/ClimateR>.

Site	Species	Location	Weather station	Meteorological parameters				Length of vegetation period (day)	Thawing permafrost depth (max, cm)	Annual air temperature (°C)	Annual precipitation (mm)
				T (°C)	P (mm)	S (h/month)	VPD (kPa)				
				Periods							
YAK	<i>Larix cajanderi</i> Mayr.	69°N, 148°E	Chokurdach 62°N, 147°E, 61 m. a.s.l.	1950-2000	1966-2000	1961-2000	1950-2000	50-70*	20-50*	-14.7	205
TAY	<i>Larix gmelinii</i> Rupr.	70°N, 103°E	Khatanga 71°N, 102°E, 33m. a.s.l.	1950-2000	1966-2000	1961-2000	1950-2000	90**	40-60**	-13.2	269
ALT	<i>Larix sibirica</i> Ledeb.	50°N, 89°E	Mugur Aksy 50°N, 90°E 1850 m. a.s.l.	1963-2000	1966-2000			90-120***	80-100***	-2.7	153
			Kosh-Agach 50°N, 88°E 1758 m.a.s.l.			1961-2000	1950-2000				

202 \*Abaimov, 1996; Hughes et al., 1999; Churakova (Sidorova) et al., 2016

203 \*\*Naurzbaev et al., 2002

204 \*\*\*Sidorova et al., 2011

205 *2.3. Tree-ring width analysis*

206 Ring width of 12 trees was re-measured for each selected period. Cross-dating was checked by  
207 comparison with the existing complete 2000-yr TRW chronologies (Fig. 1). The TRW series were  
208 standardized using the ARSTAN program (Cook and Krusic, 2008) based on the negative expo-  
209 nential curve ( $k > 0$ ) or a linear regression (any slope) prior to averaging with the bi-weight robust  
210 mean (Cook and Kairiukstis 1990). Signal strength in regional TRW chronologies was assessed  
211 with the Expressed Population Signal (EPS) statistics as it measures how well the finite sample  
212 chronology compares with a theoretical population chronology based on an infinite number of  
213 trees (Wigley et al., 1984). RBAR and EPS values of stable isotope chronologies were calculated  
214 for the period from 1950 to 2000, for which individual trees were analyzed separately, and show  
215 the common signal with an  $EPS > 0.85$ . Back in time, we used pooled material only. For all other  
216 tree-ring parameters, EPS also exceeds the threshold of 0.85.

217

218 *2.4. Image analysis of cell wall thickness (CWT)*

219 Analysis of wood anatomical features was performed for all studied periods with an AxioVision  
220 scanner (Carl Zeiss, Germany). Micro-sections were prepared using a sliding microtome and  
221 stained with methyl blue (Furst, 1979). Tracheids in each tree ring were measured along five radial  
222 files of cells (Munro et al., 1996; Vaganov et al., 2006) selected for their larger tangential cell  
223 diameter (T). For each tracheid, CWT and the radial cell diameter (D) were computed. In a second  
224 step, tracheid anatomical parameters were averaged for every tree ring. Site chronologies are pre-  
225 sented for the complete annual ring chronology without standardization due to the absence of low-  
226 frequency trend. CWT data from ALT for the periods 1790-1835 and 1950-2000 were used from  
227 the past studies (Sidorova et al., 2011; Fonti et al., 2013) and for YAK for the period from 1600-  
228 1980 from Panyushkina et al. (2003). Unfortunately, the remaining YAK sample size was too  
229 small for anatomical analyses. Thus it was impossible to produce a clear anatomical signal for the

230 CE 536 ring from existing material. As a result, cell wall thickness is missing for this year at TAY  
231 (Fig. 2).

232

### 233 2.5. Maximum latewood density (MXD)

234 Maximum latewood density chronologies from ALT were available continuously for the period  
235 CE 1407-2007 from Schneider et al. (2015) and for YAK and TAY the period CE 1790-2004 from  
236 Sidorova et al. (2010). For any of the other periods, at least six cross-sections (for CE 516-560,  
237 only four sections could be used, as this period is not as well replicated) were sawn with a double-  
238 bladed saw, to a thickness of 1.2 mm, at right angles to the fiber direction. Samples were exposed  
239 to X-rays for 35-60 min (Schweingruber 1996). MXD measurements were obtained with a reso-  
240 lution of 0.01 mm, and brightness variations transferred into ( $\text{g}\cdot\text{cm}^3$ ) using a calibration wedge  
241 (Lenz et al., 1976; Eschbach et al., 1995) from a Walesch X-ray densitometer 2003. All MXD  
242 series were detrended in ARSTAN by calculating subtractions from straight-line functions (Fritts,  
243 1976). Site chronologies were developed for each volcanic period using the bi-weight robust mean.

244

### 245 2.6. Stable carbon ( $\delta^{13}\text{C}$ ) and oxygen ( $\delta^{18}\text{O}$ ) isotopes in tree-ring cellulose

246 During photosynthetic  $\text{CO}_2$  assimilation  $^{13}\text{CO}_2$  is discriminated against  $^{12}\text{CO}_2$ , leaving the newly  
247 produced assimilates depleted in  $^{13}\text{C}$ . The carbon isotope discrimination ( $^{13}\Delta$ ) is partitioned in the  
248 diffusional component with  $a = 4.4\text{‰}$  and the biochemical fractionation with  $b = 27\text{‰}$ , for C3  
249 plants, during carboxylation via Rubisco. The  $^{13}\Delta$  is directly proportional to the  $c_i/c_a$  ratio, where  
250  $c_i$  is the leaf intercellular, and  $c_a$  the ambient  $\text{CO}_2$  concentration. This ratio reflects the balance  
251 between stomatal conductance ( $g_l$ ) and photosynthetic rate ( $A_N$ ). A decrease in  $g_l$  at a given  $A_N$   
252 results in a decrease of  $^{13}\Delta$ , as  $c_i/c_a$  decreases and vice versa. The same is true when  $A_N$  increases  
253 or decreases at a given  $g_l$ . Since  $\text{CO}_2$  and  $\text{H}_2\text{O}$  gas exchange are strongly interlinked with the C-  
254 isotope fractionation  $^{13}\Delta$  is controlled by the same environmental variables i.e. PaR,  $\text{CO}_2$ , VPD  
255 and temperature (Farquhar et al., 1982, 1989; Cernusak et al., 2013).

256 The oxygen isotopic compositions of tree-ring cellulose record the  $\delta^{18}\text{O}$  of the source water de-  
257 rived from precipitation, which itself is related to temperature variations at middle and high lati-  
258 tudes (Craig, 1961; Daansgard, 1964). It is modulated by evaporation at the soil surface and to a  
259 larger degree by evaporative and diffusion processes in leaves; the process is largely controlled by  
260 the vapor pressure deficit (Dongmann et al., 1972, Farquhar and Loyd, 1993, Cernusak et al.,  
261 2016). A further step of fractionation occurs as sugar molecules are transferred to the locations of  
262 growth (Roden et al., 2000). During the formation of organic compounds the biosynthetic frac-  
263 tionation leads to a positive shift of the  $\delta^{18}\text{O}$  values by 27‰ relative to the leaf water (Sternberg,  
264 2009). The oxygen isotope variation in tree-ring cellulose therefore reflects a mixed climate infor-  
265 mation, often dominated by a temperature, source water or sunshine duration modulated by the  
266 VPD influence.

267 The cross-sections of relict wood and cores from living trees used for the TRW, MXD and CWT  
268 measurements were then selected for the isotope analyses. We analyzed four subsamples for each  
269 studied period according to the standards and criteria described in Loader et al. (2013). The first  
270 50 yrs. of each sample were excluded to limit juvenile effects (McCarroll and Loader, 2004). After  
271 splitting annual rings with a scalpel, the whole wood samples were enclosed in filter bags.  $\alpha$ -  
272 cellulose extraction was performed according to the method described by Boettger et al. (2007).  
273 For the analyses of  $^{13}\text{C}/^{12}\text{C}$  and  $^{18}\text{O}/^{16}\text{O}$  isotope ratios, 0.2-0.3 mg and 0.5-0.6 mg of cellulose were  
274 weighed for each annual ring, into tin and silver capsules, respectively. Carbon and oxygen iso-  
275 topic ratios in cellulose were determined with an isotope ratio mass spectrometer (Delta-S, Finni-  
276 gan MAT, Bremen, Germany) linked to two elemental analyzers (EA-1108, and EA-1110 Carlo  
277 Erba, Italy) via a variable open split interface (CONFLO-II, Finnigan MAT, Bremen, Germany).  
278 The  $^{13}\text{C}/^{12}\text{C}$  ratio was determined separately by combustion under oxygen excess at a reactor tem-  
279 perature of 1020°C. Samples for  $^{18}\text{O}/^{16}\text{O}$  ratio measurements were pyrolyzed to CO at 1080°C  
280 (Saurer et al., 1998). The instrument was operated in the continuous flow mode for both, the C and

281 O isotopes. The isotopic values were expressed in the delta notation multiplied by 1000 relative to  
 282 the international standards (Eq. 1):

$$283 \quad \delta \text{ sample} = R_{\text{sample}}/R_{\text{standard}}-1 \quad (\text{Eq. 1})$$

284 where  $R_{\text{sample}}$  is the molar fraction of  $^{13}\text{C}/^{12}\text{C}$  or  $^{18}\text{O}/^{16}\text{O}$  ratio of the sample and  $R_{\text{standard}}$  the molar  
 285 fraction of the standards, Vienna Pee Dee Belemnite (VPDB) for carbon and Vienna Standard  
 286 Mean Ocean Water (VSMOW) for oxygen. The precision is  $\sigma \pm 0.1\%$  for carbon and  $\sigma \pm 0.2\%$   
 287 for oxygen. To remove the atmospheric  $\delta^{13}\text{C}$  trend after CE 1800 from the carbon isotope values  
 288 in tree rings (i.e. Suess effect, due to fossil fuel combustion) we used atmospheric  $\delta^{13}\text{C}$  data from  
 289 Francey et al. (1999), <http://www.cmdl.noaa.gov/info/ftpdata.html>). These corrected series were  
 290 used for all statistical analyses. The  $\delta^{18}\text{O}$  cellulose series were not detrended.

291

## 292 *2.7. Climatic data*

293 Meteorological series were obtained from local weather stations close to the study sites and used  
 294 for the computation of correlation functions between tree-ring proxies and monthly climatic pa-  
 295 rameters (Table 2). Sunshine duration data were obtained from available Kosh-Agach meteoro-  
 296 logical station (<http://aisori.meteo.ru/ClimateR>).

297

## 298 *2.8. Statistical analysis*

299 All chronologies for each period were normalized to z-scores (Fig. 2). To assess post-volcanic  
 300 climate variability, we used Superposed Epoch Analysis (SEA, Panofsky and Brier, 1958) with  
 301 the five proxy chronologies available at each of the three study sites. In this experiment, the 15  
 302 years before and after a volcanic eruption were analyzed. SEA is applied to the six annually dated  
 303 volcanic eruptions (Table 1).

304 To test the sensitivity of the studied tree-ring parameters to climate, bootstrap correlation functions  
 305 have been computed between proxy chronologies and monthly climate predictors using the  
 306 ‘bootRes’ package of R software (R Core Team 2016) for the period 1950 (1966)-2000.

307 To estimate whether volcanic years can be considered as extreme, we computed Probability Den-  
308 sity Functions (PDFs, Stirzaker, 2003) for each study site and for each tree-ring parameter over a  
309 period of 221 years for which measurements are available (Fig. S1). A year is considered (very)  
310 extreme if the value of a given parameter is below the (5<sup>th</sup>) 10<sup>th</sup> percentile of the PDF. We applied  
311 unpaired t-test statistics to check significance between each proxy and each site.

312

### 313 3. Results

#### 314 3.1. Anomalies in tree-ring proxy chronologies after stratospheric volcanic eruptions

315 Normalized TRW chronologies show negative deviations the year following the eruptions at YAK  
316 and ALT with significant anomalies in CE 536 (-2.7  $\sigma$  and -1.8  $\sigma$  for YAK and ALT respectively)  
317 and a delayed decrease, two years after the events, at TAY (Fig. 2). Regarding CWT, a strong  
318 decrease is observed in CE 536 at YAK. Only two layers of cells were formed in CE 536 as com-  
319 pared to the 11-20 layers of cells formed on average during “normal” years. In addition, we also  
320 observe the formation of frost rings in ALT between CE 536 and 538, as well as in 1259.

321 Furthermore, we reveal decreasing MXD values for ALT (-4.4  $\sigma$ ) and YAK (-2.8  $\sigma$ ) were observed  
322 in CE 537. However, for TAY, we found less pronounced patterns of variation (Fig. 2). In this  
323 regard, the sharpest decrease is observed in the CWT chronologies from YAK (-3.9 $\sigma$ ) in CE 541,  
324 as well as in TAY (-3.0  $\sigma$ ) and ALT (- 2.9  $\sigma$ ) one and two years, respectively after the eruptions  
325 (Fig. 2). The  $\delta^{18}\text{O}$  chronologies show a distinct decrease one year after the eruptions for YAK -  
326 3.9  $\sigma$ , in the year of 1259, TAY -3.0 $\sigma$  in 537, and ALT - 2.9  $\sigma$  in 537 only (Fig. 2, Fig. S1). Finally,  
327  $\delta^{13}\text{C}$  negative anomalies are observed in TAY, and – to a lesser extent – in YAK two years after  
328 almost all of the eruptions, but are largely absent from the ALT chronology. The CE 540 eruption  
329 was recorded in CWT and  $\delta^{13}\text{C}$  at YAK only (Fig. 2). With respect to the CE 1257 Samalas erup-  
330 tion (Fig. 2), the year following the eruption was recorded as very extreme in the TRW and CWT  
331 chronologies at all sites whereas very extreme anomalies were recorded in  $\delta^{13}\text{C}$  for CE 1259 (see  
332 Fig. S1).



333

**YAK**

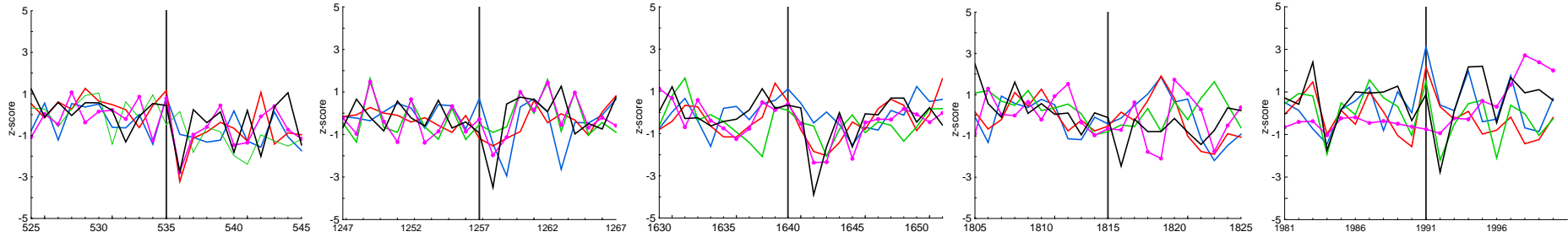
**CE 535**

**CE 1257**

**CE 1640**

**CE 1815**

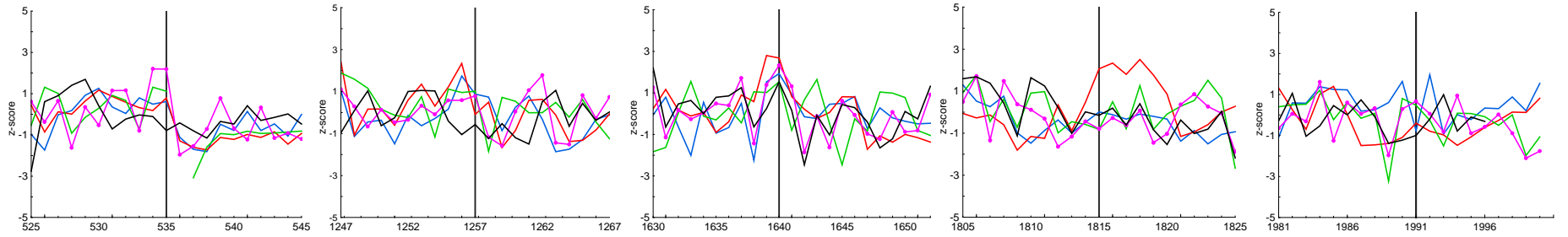
**CE 1991**



334

335

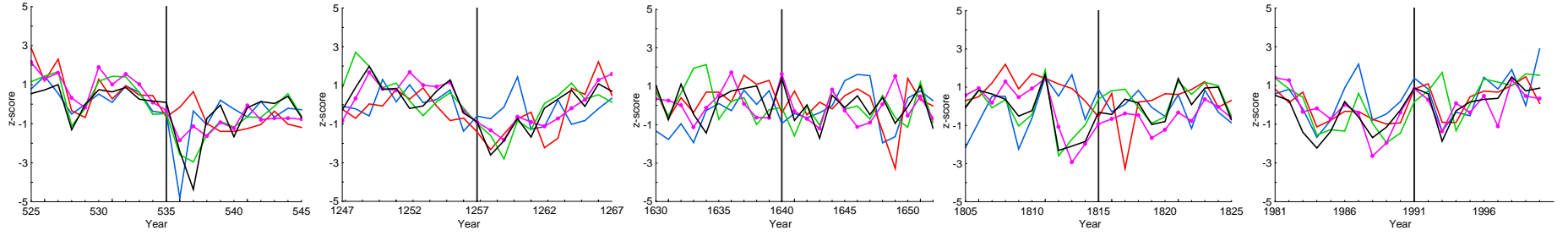
**TAY**



336

337

**ALT**



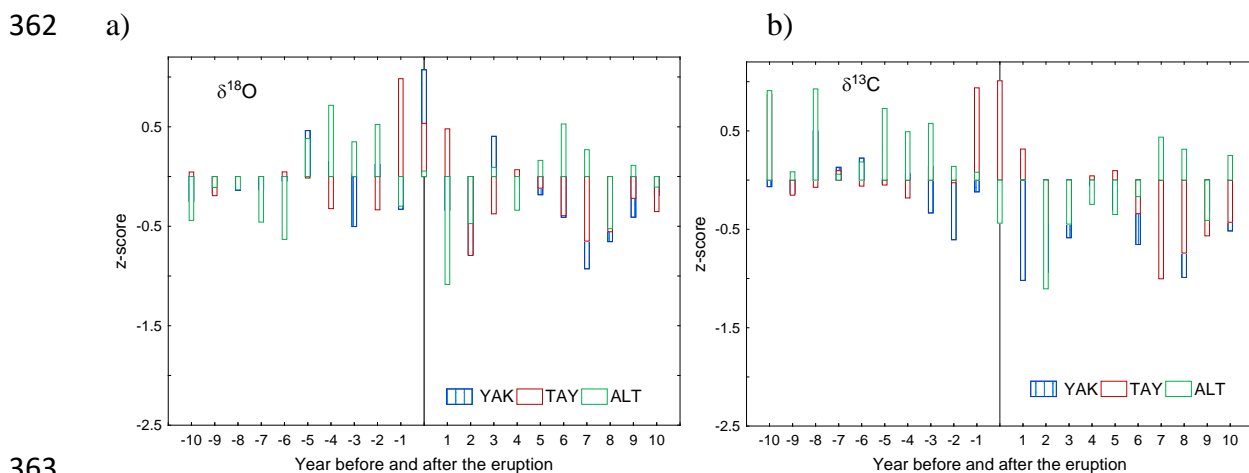
338

339

340 **Fig. 2.** Normalized (z-score) individual tree-ring index chronologies (TRWi, pink), maximum latewood density (MXD, black), cell wall thick-  
 341 ness (CWT, green),  $\delta^{13}\text{C}$  (red) and  $\delta^{18}\text{O}$  (blue) in tree-ring cellulose chronologies from YAK, TAY and ALT for the specific periods 10 years  
 342 before and after the eruptions CE 535, 1257, 1640, 1815 and 1991 are presented. Vertical lines showed year of the eruptions.

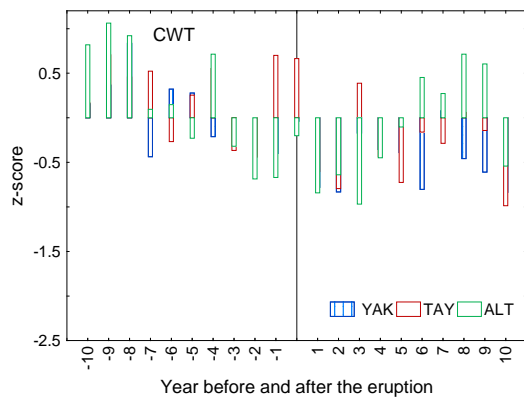
343

344 The impacts of the more recent CE 1640 Parker, 1815 Tambora, and 1991 Pinatubo eruptions  
 345 are, by contrast, by far less obvious. In CE 1643, extreme decreases are observed in the TRW  
 346 and CWT series of the high-latitude sites YAK and TAY, whereas tree-ring proxies are not  
 347 clearly affected at ALT. No extreme anomalies are observed in CE 1816 in Siberia regardless  
 348 of the site and the tree-ring parameter analyzed. The ALT  $\delta^{13}\text{C}$  chronology can be seen as an  
 349 exception to the rule here as it evidenced extreme values in CE 1817. Finally, the Pinatubo  
 350 eruption is captured in CE 1992 by MXD and CWT chronologies from YAK and classified as  
 351 extreme in the CWT and  $\delta^{18}\text{O}$  chronologies from ALT in 1993 (Fig. S1, right panel).  
 352 Overall, the SEA (Fig. 3) shows the high spatiotemporal variability and complexity of the re-  
 353 sponse of the Siberian climate system to the largest volcanic events over past millennium (CE  
 354 535, 1257, 1641, 1815 and 1991). A lagged response by one year after the eruptions is observed  
 355 in the CWT proxies at all three sites (Fig. 3c). The behavior of isotope chronologies is rather  
 356 more complex, with a distinct decrease in  $\delta^{13}\text{C}$  (Fig. 3b) at the high-latitude sites (YAK, TAY),  
 357 whereas  $\delta^{18}\text{O}$  series (Fig. 3a) are impacted mainly at the high-altitude ALT site. We find sig-  
 358 nificant differences ( $p=0.014$ ,  $df=40$ ,  $n=21$ ) between averaged  $\delta^{13}\text{C}$  chronologies of the YAK  
 359 and ALT sites. SEA for TRW (Fig. 3d) and MXD (Fig. 3e) show a more drastic decrease of  
 360 values during the first year, mainly for YAK, when compared to other proxies and study sites  
 361 (Fig. 3 a,b,c).

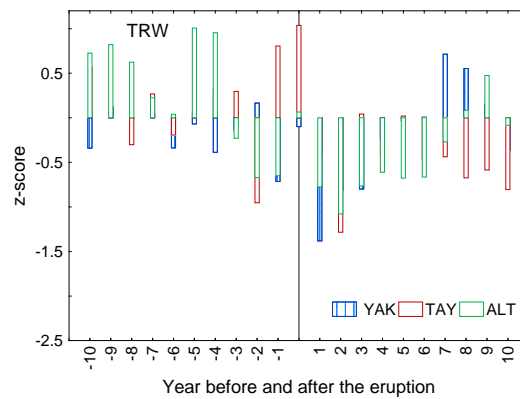


363  
364

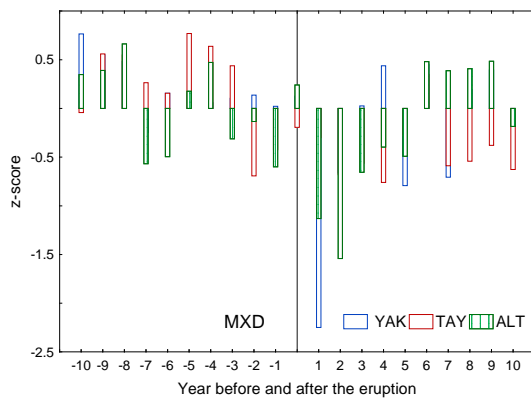
365 c)



d)

366  
367

e)

368  
369

**Fig. 3.** Superposed epoch analysis of  $\delta^{18}\text{O}$  (a),  $\delta^{13}\text{C}$  (b), CWT (c), TRW (d) and MXD (e)

370 chronologies for each study site and for the major volcanic eruptions in CE 535, 1257, 1641,  
371 1815 and 1991.

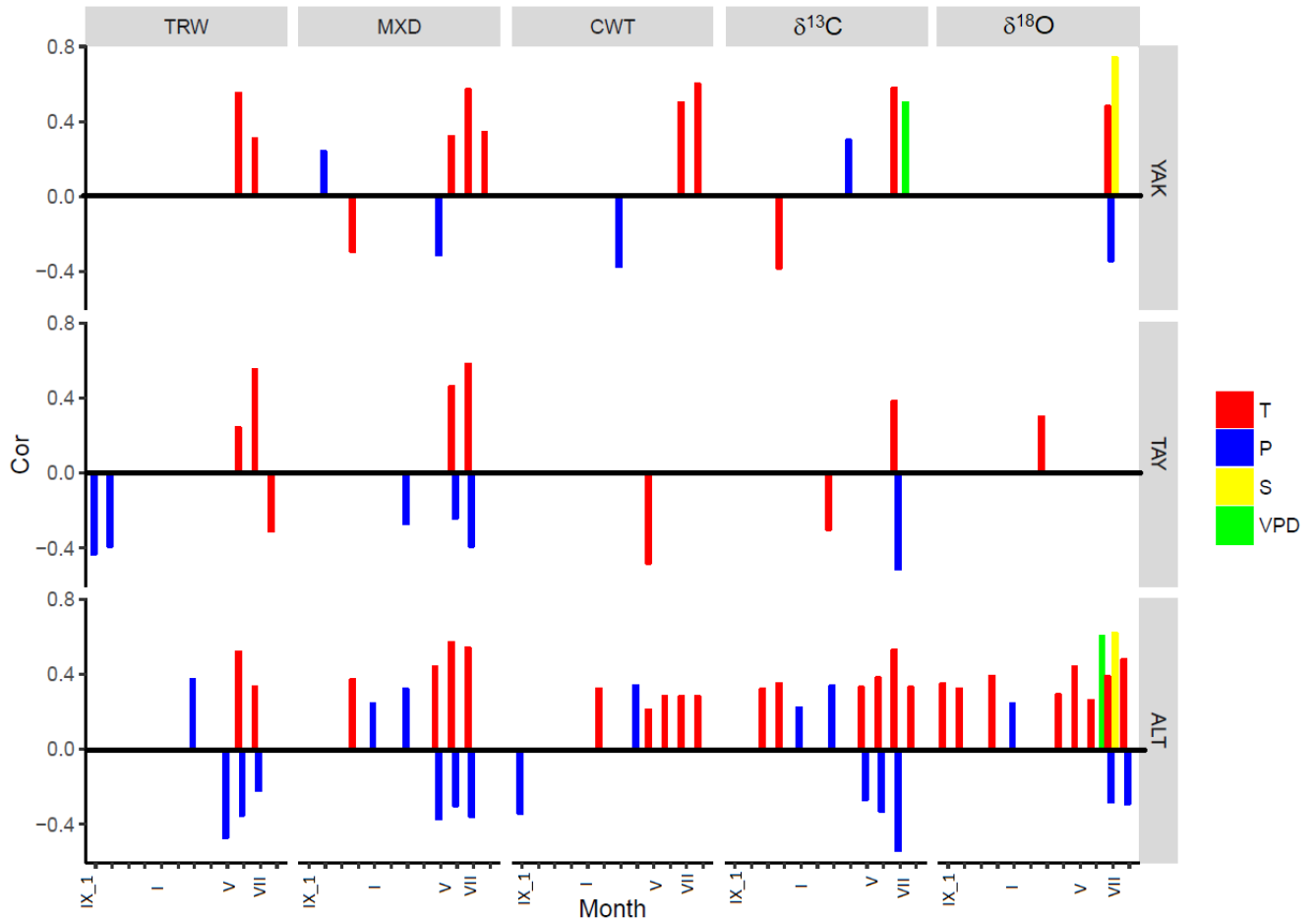
372

### 373 3.2. Tree-ring proxies versus meteorological series

374

#### 375 3.2.1. Monthly air temperatures and sunshine duration

376 Bootstrapped functions evidence significant positive correlations ( $p < 0.05$ ) between TRW and  
377 MXD chronologies and mean summer (June-July) temperatures at all sites. Temperatures at the  
378 beginning (June) and the end of the growing season (mid-August) influenced the MXD chro-  
379 nology in ALT ( $r = 0.57$ ) and YAK ( $r = 0.55$ ), respectively (Fig. 4). July temperatures appear  
380 as a key factor for determining tree growth as they significantly impact CWT,  $\delta^{13}\text{C}$ , and  $\delta^{18}\text{O}$   
381 (with the exception of TAY for the latter) chronologies ( $r = 0.28$ - $0.60$ ) at YAK and ALT.



382  
 383 **Fig. 4.** Significant correlation coefficients between tree-ring parameters: TRW, MXD, CWT,  
 384 δ<sup>13</sup>C and δ<sup>18</sup>O versus weather station data: temperature (T, red), precipitation (P, blue), vapor  
 385 pressure deficit (VPD, green), and sunshine duration (S, yellow) from September of the previ-  
 386 ous year to August of the current year for three study sites were calculated. Table 2 lists stations  
 387 used in the analysis.

388  
 389 Namely, February and March temperatures affected significantly δ<sup>18</sup>O as recorded in the cellu-  
 390 lose chronologies at YAK, ALT (r=0.25, r=0.26), while March and May (r=0.30) temperatures  
 391 in TAY, respectively.

392 Correlation analysis between July temperature and July sunshine duration showed significant  
393 correlation for YAK ( $r=0.56$ ) and ALT ( $r=0.34$ ). July sunshine duration are strongly and posi-  
394 tively correlated with  $\delta^{18}\text{O}$  in larch tree-ring cellulose chronologies from YAK ( $r=0.73$ ) and  
395 ALT ( $r=0.51$ ) for the period 1961-2000.

396

### 397 *3.2.2. Monthly precipitation*

398 The strongest July precipitation signal is observed at ALT ( $r=-0.54$ ) and TAY ( $r=-0.51$ ) with  
399  $\delta^{13}\text{C}$  chronologies ( $p<0.05$ ). In addition, at ALT a positive relationship is observed between  
400 March precipitation and TRW ( $p<0.05$ ) ( $r=0.37$ ), MXD ( $r=0.32$ ) and CWT ( $r=0.34$ ), respec-  
401 tively. At YAK, July precipitation showed negative relationship with  $\delta^{18}\text{O}$  in tree-ring cellulose  
402 ( $r=-0.34$ ;  $p<0.05$ ) only.

403

### 404 *3.2.3. Vapor pressure deficit (VPD)*

405 June VPD is significantly and positively correlated with the  $\delta^{18}\text{O}$  chronology from ALT ( $r=0.67$   
406  $p<0.05$ , respectively) for the period 1950-2000. The  $\delta^{13}\text{C}$  in tree-ring cellulose from YAK cor-  
407 relate with July VPD only ( $r=0.69$   $p<0.05$ ). We did not find a significant influence of VPD in  
408 TAY tree-ring and stable isotope parameters.

409

### 410 *3.2.4. Synthesis of the climate data analysis*

411 In summary, we found that during the instrumental period of weather station observations (Ta-  
412 ble 2) mainly summer temperature influenced TRW, MXD and CWT from the HL sites (YAK,  
413 TAY), while stable carbon and oxygen isotopes were affected by summer precipitation (YAK,  
414 TAY, ALT), sunshine duration (YAK, ALT), and vapor pressure deficit (YAK, ALT) signals.

415

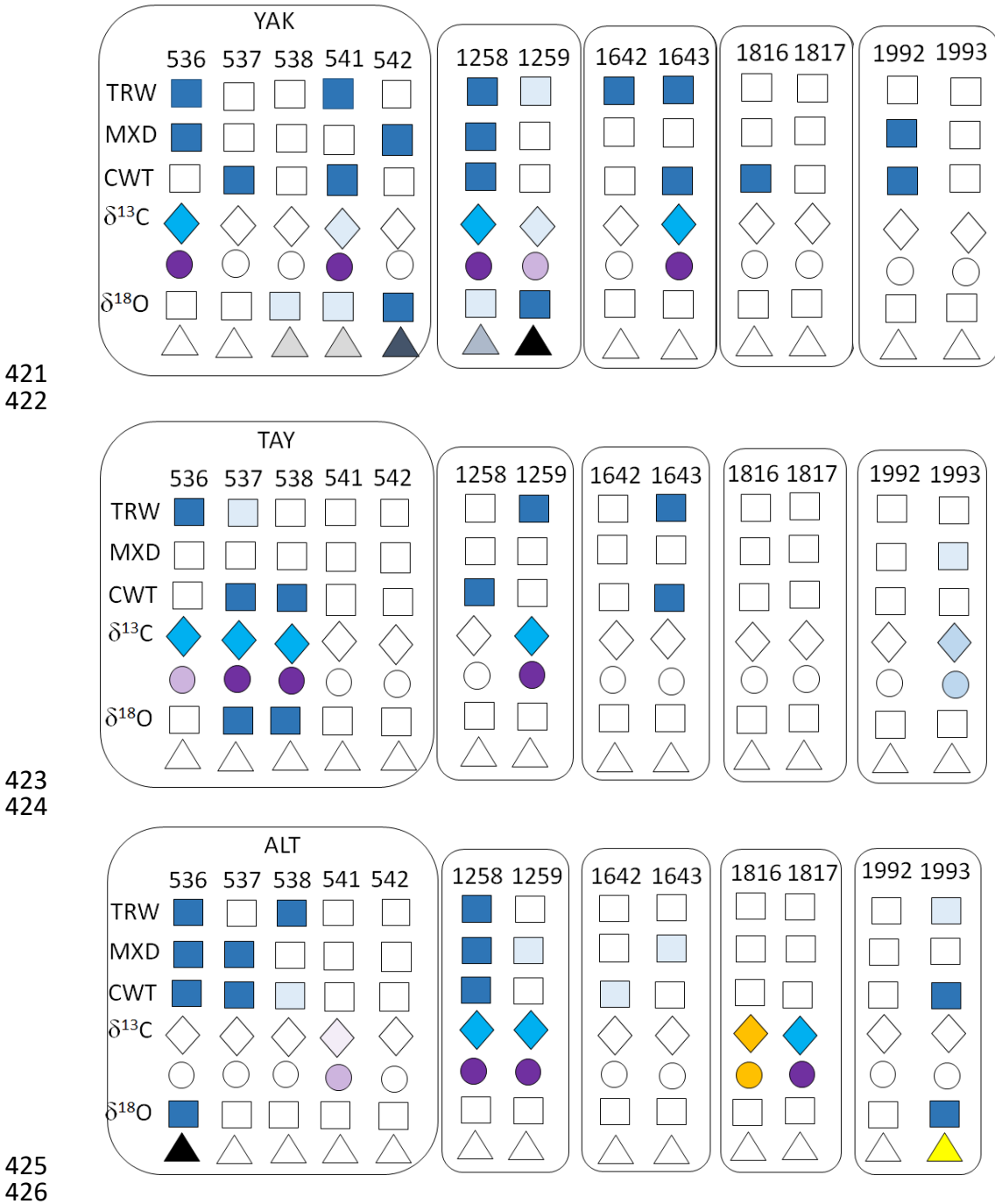
416

417 3.3. Response of Siberian larch trees to climatic changes after the major volcanic eruptions

418 Based on the statistical analysis above for the calibration period, we assumed that these rela-

419 tionships would not change over time and will provide information about climatic changes dur-

420 ing past volcanic periods (Fig. 5).



427 **Fig. 5.** Response of larch trees from Siberia to the CE volcanic eruptions (Table 1) with per-

428 centile of distribution considered as very extreme (<5th, intensive color), extreme (>5th, <10th,

429 light color) and non-extreme (>10th, white color). July temperature changes presented as a  
430 square from **heavy blue** (cold) to **light blue** (moderate). Summer vapor pressure deficit (VPD)  
431 variabilities are shown as a circle from **purple** (low), **light purple** (moderate decrease) to **or-**  
432 **ange** (increase, developing to dry air). July precipitation presented as a rhomb from **heavy tur-**  
433 **quoise** (wet), **light blue** (moderate) to **orange** (dry). Low July sunshine duration shown as  
434 black triangle, while high – as yellow.

435

### 436 *3.3.1. Temperature proxies*

437 We found strong summer air temperature anomalies at all sites after the 535 and 1257 CE vol-  
438 canic eruptions. The temperature decrease was found in the TRW and CWT datasets at all sites,  
439 and also in the MXD datasets at YAK and ALT (Fig. 5). For the volcanic eruptions in later  
440 centuries, the evidence for a decrease in temperature was not as pronounced. Namely, no strong  
441 drop in summer temperature was found for ALT in CE 1642 nor 1643, an extreme cold in TAY  
442 for 1643 only, while still a cold summer in YAK for both years; 1816 was cold only in YAK  
443 (based on the CWT chronology), but not at the other sites. CE 1992 was recorded as a cold year  
444 based on MXD and CWT from YAK, but again not for the other sites; CE 1993 was an extreme  
445 year for ALT based on CWT and  $\delta^{18}\text{O}$ .

446

### 447 *3.3.2. Moisture proxies: precipitation and VPD*

448 Based on the climatological analysis with the local weather stations data (Table 2, Fig. 4) for  
449 all studied sites we considered  $\delta^{13}\text{C}$  in cellulose chronologies as proxies for precipitation  
450 changes. Yet, CWT from ALT could be considered as a proxy with mixed temperature and  
451 precipitation signal (Fig. 4, Fig. 5). Therefore, CE 536 was extremely humid in YAK and TAY,  
452 as well as 541 and 542 in TAY and ALT. CE 1258 was dry in YAK and ALT, while drier than  
453 normal conditions occurred in 1259 for all studied sites. CE 1641 was dry in TAY; 1642 in

454 YAK and ALT. A rather wet summer was in TAY during 1815 and 1816 years. CE 1991 was  
455 wet in YAK, 1992 in ALT followed by a dry summer in 1993 (Fig. 5).

456

### 457 *3.3.3. Sunshine duration proxies*

458 Instrumental measurements of sunshine duration (Table 2) in YAK and ALT during the recent  
459 period showed a significant link with  $\delta^{18}\text{O}$  cellulose. Based on this we conclude that sunshine  
460 duration decreased significantly in 536, 541, 542, 1258 and 1259 in YAK, and 536 in ALT.  
461 Conversely, summer 1993 in ALT was very sunny (Fig. 5).

462

## 463 **4. Discussion**

464 In this paper, we analyze climatic anomalies in years following selected, large volcanic erup-  
465 tions of the CE using long-term, tree-ring multi-proxy chronologies for  $\delta^{13}\text{C}$  and  $\delta^{18}\text{O}$ , TRW,  
466 MXD, CWT for the high-latitude (YAK, TAY) and high-altitude (ALT) sites. The main goal  
467 was to explore the suitability of the above-mentioned proxies for the detection of abrupt cli-  
468 matic changes caused by volcanic eruptions: (i) for each proxy alone, and (ii) for the combined  
469 use of all proxies, to reconstruct the respective climatic changes, which should go beyond tem-  
470 perature. Since trees as living organisms respond to various climatic impacts, the carbon assim-  
471 ilation and growth patterns accordingly leave unique “finger prints” in the photosynthates,  
472 which is recorded in the wood of the tree rings specifically and individually for each proxy.

473

### 474 *4.1. Evaluation of the applied proxies in Siberian tree-ring data*

475 This study clearly shows that each proxy has to be analyzed and interpreted specifically for its  
476 validity on each studied site and evaluated for its suitability for the reconstruction of abrupt  
477 climatic changes.



478 TRW in temperature-limited environments is a proxy for summer temperature reconstructions,  
479 as growth is a temperature-controlled process. Temperature clearly determines the duration of  
480 the growing season and the rate of cell division (Cuny et al., 2014). Accordingly, low growing  
481 season temperatures are reflected in narrow tree rings. The upper temperature limit is species  
482 and biome specific. In most cases tree growth is limited by drought rather than by high temper-  
483 atures, since water shortage and VPD increase with increasing temperature. Still this does not  
484 make TRW a suitable proxy to determine the influence of water availability and air humidity,  
485 especially at the temperature-limited sites.

486 MXD chronologies obtained for the Eurasian subarctic record mainly a July-August tempera-  
487 ture signal (Vaganov et al., 1999; Sidorova et al., 2010; Büntgen et al., 2016) and add valuable  
488 information about climate conditions toward the end of the growth season. Similarly, CWT is  
489 an anatomical parameter, which contains information on carbon sink limitation of the cambium  
490 due to extreme cold conditions (Panyushkina et al., 2003; Fonti et al., 2013; Bryukhanova et  
491 al., 2015). The clear signal about reduced number of cells within a season, for example, strong  
492 decreasing CWT in CE 536 at YAK or formation of frost rings in ALT (CE 536-538, 1259) has  
493 been shown in our study.

494 Low  $\delta^{13}\text{C}$  values can be explained by a reduction in photosynthesis caused by volcanic dust  
495 veils. For the distinction whether  $\delta^{13}\text{C}$  is predominantly determined by  $A_N$  or  $g_l$  the combined  
496 evaluation with  $\delta^{18}\text{O}$  or TRW is needed. High  $\delta^{18}\text{O}$  values indicate high VPD, which induces a  
497 reduction in stomatal conductance, reducing the back diffusion of depleted water molecules  
498 from the ambient air. This confirms a sunny year CE 1991 in YAK and to some extent in ALT  
499 with warm and dry weather conditions. Interestingly, we also find less negative values for  $\delta^{13}\text{C}$   
500 in the same period. This shows that the two isotopes correlate with each other and this indicates  
501 the need for a combined evaluation of the C and O isotopes (Scheidegger et al., 2000) taking  
502 into account precautions as suggested by Roden and Siegwolf (2012).

503 *4.2. Lag between volcanic events and response in tree rings*

504 In most of the discussed events, we observe a certain delay – or lag – between the eruption and  
505 the response in tree rings of one year or more (Fig. 3). This lag is explained by the tree's use of  
506 stored carbohydrates, which are the substrate for needle and early wood production. These  
507 stored carbohydrates carry the isotopic signal of previous years and depending on their remo-  
508 bilization and use mask the signals in freshly produced biomass. The delayed signal could also  
509 reflect the time needed for the dust veil to be transported to the study sites.

510

511 *4.3. Temperature and sunshine duration changes after stratospheric volcanic eruptions*

512 Correlation functions show that MXD and CWT (with the exception of TAY in the latter case),  
513 and to a lesser extent also TRW chronologies, portray the strongest signals for summer (June-  
514 August) temperatures. In addition, significant information about sunshine duration can be de-  
515 rived from the YAK and ALT  $\delta^{18}\text{O}$  series. Thus, we hypothesize that extremely narrow TRW  
516 and very negative anomalies observed in the MXD and CWT chronologies of YAK and to a  
517 lesser extent at ALT, in CE 536 and 1258 along with low  $\delta^{18}\text{O}$  values (except for ALT in CE  
518 1257) reflect cold conditions in summer. Presumably, the temperatures were below the thresh-  
519 old values for growth (Körner, 2015). This hypothesis of a generalized regional cooling after  
520 both eruptions is further confirmed by the occurrence of frost rings at all sites in CE 536  
521 (Myglan et al., 2008; Guillet et al., 2017), as well as in neighboring Mongolia (D'Arrigo et al.,  
522 2001). The unusual cooling in CE 536 is also evidenced by a very small number of cells formed  
523 at YAK (Churakova (Sidorova) et al., 2014). According to the CWT chronologies, this cooling  
524 likely persisted throughout the region in CE 537 and was limited to TAY and ALT in CE 538  
525 with formation of frost rings in ALT. Although  $\delta^{18}\text{O}$  is an indirect proxy for needle temperature,  
526 low  $\delta^{18}\text{O}$  values in CE 536 and 1258 for YAK and ALT are a result of low irradiation, leading

527 to low temperature and low VPD (high stomatal conductance), both likely a result from volcanic  
528 dust veils.

529 Similarly, in the aftermath of the Samalas eruption, the persistence of summer cooling is limited  
530 to CE 1259 only at the three study sites, which is in line with findings of Guillet et al., (2017).  
531 Interestingly, a slight decrease in oxygen isotope chronologies – which can be related to low  
532 levels of summer sunshine duration (i.e. low leaf temperatures) – allows for hypothesizing that  
533 cool conditions could have prevailed.

534 For all later high-magnitude CE eruptions, temperature-sensitive tree-ring proxies do not evi-  
535 dence a generalized drop in summer temperatures. Paradoxically, the impacts of the Tambora  
536 eruption, known for its triggering of a widespread “year without summer” (Harrington, 1992),  
537 did only induce abnormal CWT at YAK, but no anomalies are observed at sites TAY and ALT,  
538 except for the positive deviation of  $\delta^{13}\text{C}$  (Fig. 2). While these findings may seem surprising,  
539 they are in line with the TRW and MXD reconstructions of Briffa et al., (1998) or Guillet et al.,  
540 (2017), who found limited impacts of the CE 1815 Tambora event in Eastern Siberia and Alaska  
541 using TRW and MXD data only. The inclusion of CWT chronologies, not used in their recon-  
542 structions, further confirm the absence of a significant cooling in this region following the sec-  
543 ond largest eruption of the last millennium.

544 Finally, in CE 1992, our results evidence cold conditions in YAK, which is consistent with  
545 weather observations showing that the below-average anomalies in summer temperatures (after  
546 Pinatubo eruption) were indeed limited to Northeastern Siberia (Robock, 2000). As both iso-  
547 topes indicate a reduction in stomatal conductance, we found that warm (in agreement with  
548 MXD and CWT) and dry conditions were prevalent for YAK and ALT at this time. This iso-  
549 topic constellation was confirmed by the positive relationships between VPD and  $\delta^{18}\text{O}$  and  $\delta^{13}\text{C}$   
550 for YAK and ALT.

551 However, temperature and sunshine duration are not always highly coherent over time due to  
552 the influence of other factors, like Arctic Oscillations as it was suggested for Fennoscandia  
553 regions by Loader et al. (2013).

554

#### 555 *4.4. Moisture changes*

556 Water availability is a key parameter for Siberian trees as they are growing under extremely  
557 continental conditions with hot summers and cold winters, and even more so with very low  
558 annual precipitation (Table 2). Continuous permafrost, in addition, is playing a crucial role, and  
559 can be considered as a buffer for additional water sources during hot summers (Sugimoto et al.,  
560 2002; Boike et al., 2013; Saurer et al., 2016). Yet, thawed permafrost water is not always avail-  
561 able for roots due to the surficial structure of the root plate or extremely cold water temperature  
562 (close to 0°C), which can hardly be utilized by trees (Churakova (Sidorova) et al., 2016). Thus,  
563 Siberian trees are highly susceptible to drought, induced by dry and warm air during July and  
564 therefore the stable carbon isotopes can be sensitive indicators of such conditions. After vol-  
565 canic eruptions, however, low light intensity due to dust veils induce low temperatures and  
566 reduced VPD, the driver for evapotranspiration. Under such conditions drought stress is un-  
567 likely to occur. However, the transition phases with changes from cool and moist to warm and  
568 dry conditions are more critical when drought is more likely to occur.

569 In our study, higher  $\delta^{13}\text{C}$  values in tree-ring cellulose indicate increasing drought conditions as  
570 a consequence of reduced precipitation for two years after the CE 1257 volcanic eruption at all  
571 three sites. A local drought developed at YAK at the beginning of CE 1643, while a shift to  
572 dryer conditions was observed at TAY in the beginning of summer CE 1815 until 1820. No  
573 further extreme hydro-climatic anomalies occurred at Siberian sites in the aftermath of the  
574 Pinatubo eruption.

575

576 *4.5. Synthesized interpretation from the multi-parameter tree-ring proxies*

577 Our analysis demonstrates the added value of a tree-ring derived multi-proxy approach to better  
578 capture the climatic variability after large volcanic eruptions. Besides the well-documented ef-  
579 fects of temperature derived from TRW and MXD, CWT, stable carbon and oxygen isotopes  
580 in tree ring cellulose provide important and complementary information about moisture and  
581 sunshine duration changes (an indirect proxy for leaf temperature effective for air-to-leaf VPD)  
582 after stratospheric volcanic eruptions.

583 In detail, our results reveal a complex behavior of the Siberian climatic system to the largest  
584 eruptions of the Common Era. The CE 535 and CE 1257 Samalas eruptions caused substantial  
585 cooling – very likely induced by dust veils (Churakova (Sidorova) et al., 2014; Guillet et al.,  
586 2017; Helama et al., 2018) – as well as humid conditions at the high-latitude sites. Conversely,  
587 only local climate responses were observed after the CE 1641 Parker, 1815 Tambora, and 1991  
588 Pinatubo eruptions. Similar site-dependent impacts were found in CE 1453, 1458 and 1601  
589 (Fig. S1), frequently referred to as the coldest summers of the last millennium in the Northern  
590 Hemisphere based on TRW and MXD reconstructions (Schneider et al., 2015; Stoffel et al.,  
591 2015; Wilson et al., 2016; Guillet et al., 2017). This absence of widespread and intense cooling  
592 or reduction of precipitation over vast regions of Siberia may result from the location and  
593 strength of the volcanic eruption, atmospheric transmissivity as well as from the modulation of  
594 radiative forcing effects by regional climate variability. These results are consistent with other  
595 regional studies, which interpreted the spatio-temporal heterogeneity of tree responses to past  
596 volcanic events (Wiles et al., 2014; Esper et al., 2017; Barinov et al., 2018) in terms of regional  
597 climate peculiarities.

598

599

600

601 **5. Conclusions**

602 In this study, we demonstrate that the consequences of volcanic eruptions on climate are com-  
603 plex and heterogeneous between sites and among events. That said, we also show that each  
604 proxy alone can not provide the full information on an eruption but that it contributes to the  
605 understanding and the full picture by adding to a single, specific factor, which is critical for a  
606 comprehensive description of climate dynamics induced by volcanism and the inclusion of  
607 these phenomena in global climate models. Therefore, the application of a multiple tree-ring  
608 parameter approach provides much more detailed information. The multi-proxy approach al-  
609 lows refining the interpretation and improves our understanding of the heterogeneity of climatic  
610 signals after CE stratospheric volcanic eruptions, which are recorded in multiple tree-ring and  
611 stable isotope parameters from the vast Siberian regions.

612

613 **Author contribution:** TRW analysis was performed at V.N. Sukachev Institute of Forest SB  
614 RAS by O.V. Churakova (Sidorova), D.V. Ovchinnikov, V.S. Myglan and O.V. Naumova.  
615 CWT analysis was carried out at the V. N. Sukachev Institute of Forest SB RAS, Krasnoyarsk,  
616 Russia by M. Fonti and at the University of Arizona by I. Panyushkina. Stable isotope analysis  
617 was conducted at the Paul Scherrer Institute (PSI), by O. V. Churakova (Sidorova), M. Saurer,  
618 and R. Siegwolf. MXD measurements were realized with a DENDRO Walesh 2003 densitome-  
619 ter at WSL and at the V.N. Sukachev Institute of Forest SB RAS, Krasnoyarsk, Russia by O.  
620 V. Churakova (Sidorova) and A. V. Kirilyanov. Samples from YAK and TAY were collected  
621 by M. M. Naurzbaev. All authors contributed significantly to the data analysis and paper writ-  
622 ing.

623 **Acknowledgements:** This work was supported by Marie Curie International Incoming Fellow-  
624 ship [EU\_ISOTREC 235122], Re-Integration Marie Curie Fellowship [909122] and UFZ  
625 scholarship [2006], RFBR [09-05-98015\_r\_sibir\_a] granted to Olga V. Churakova (Sidorova);

626 SNSF M. Saurer [200021\_121838/1]; Era.Net RUSPlus project granted to M. Stoffel [SNF  
627 IZRPZO\_164735] and RFBR [№ 16-55-76012 Era\_a] granted to E.A. Vaganov; project granted  
628 to Vladimir S. Myglan RNF, Russian Scientific Fond [№ 15-14-30011]; Alexander V. Kirnya-  
629 nov was supported by the Ministry of Education and Science of the Russian Federation  
630 [#5.3508.2017/4] and RSF [#14-14-00295]; Scientific School [3297.2014.4] granted to Eugene  
631 A. Vaganov; and US National Science Foundation (NSF) grants [#9413327, #970966,  
632 #0308525] to Malcolm K. Hughes and US CRDF grant # RC1-279, to Malcolm K. Hughes  
633 and Eugene A. Vaganov. We thank Tatjana Boetgger for her support and access to the stable  
634 isotope facilities within UFZ Haale/Saale scholarship 2006; Anne Verstege, Daniel Nievergelt  
635 for their help with sample preparation for the MXD and Paolo Cherubini for providing lab  
636 access at the Swiss Federal Institute for Forest, Snow and Landscape Research (WSL).

637

638

639 **Figure legend**

640

641 **Fig. 1.** Map with the locations of the study sites (stars) and volcanic eruptions (black dots)  
642 considered in this study (a). Annual tree-ring width index (light lines) and smoothed by 51-year  
643 Hamming window (bold lines) chronologies from northeastern Yakutia (YAK - **blue**, b)  
644 (Hughes *et al.*, 1999; Sidorova 2003), eastern Taimyr (TAY - **green**, c) (Naurzbaev *et al.*,  
645 2002), and Russian Altai (ALT - **red**, d) (Myglan *et al.*, 2009) were constructed based on larch  
646 trees (Photos: V. Myglan – ALT, M. M. Naurzbaev – YAK, TAY).

647

648 **Fig. 2.** Normalized (z-score) individual tree-ring index chronologies (TRWi, **pink**), maximum  
649 latewood density (MXD, **black**), cell wall thickness (CWT, **green**),  $\delta^{13}\text{C}$  (**red**) and  $\delta^{18}\text{O}$  (**blue**)  
650 in tree-ring cellulose chronologies from YAK, TAY and ALT for the specific periods 10 years  
651 before and after the eruptions CE 535, 1257, 1640, 1815 and 1991 are presented. Vertical lines  
652 showed year of the eruptions.

653

654 **Fig. 3.** Superposed Epoch Analysis (SEA) of  $\delta^{18}\text{O}$  (a),  $\delta^{13}\text{C}$  (b), CWT (c), TRW (d) and MXD  
655 (e) chronologies for each study site by combination of the major volcanic eruptions CE 535,  
656 1257, 1641, 1815 and 1991.

657

658 **Fig. 4.** Significant correlation coefficients between tree-ring parameters and weather station  
659 data: temperature (**red**), precipitation (**blue**), vapor pressure deficit (**green**), and sunshine du-  
660 ration (yellow) from September of the previous year to August of the current year for three  
661 study sites were calculated. Table 2 lists stations used in the analysis.

662



663 **Fig. 5.** Response of larch trees from Siberia to the CE volcanic eruptions (Table 1) with per-  
664 centile of distribution considered as very extreme (< 5th, intensive color), extreme (>5th, <10th,  
665 light color) and non-extreme (>10th, white color). July temperature changes presented as a  
666 square from **heavy blue** (cold) to **light blue** (moderate). Summer vapor pressure deficit (VPD)  
667 variabilities are shown as a circle from **purple** (low), **light purple** (moderate decrease) to **or-**  
668 **ange** (increase, developing to dry air). July precipitation presented as a rhomb from **heavy tur-**  
669 **quoise** (wet), **light blue** (moderate) to **orange** (dry). Low July sunshine duration shown as  
670 black triangle, while high – as yellow.

671

672 **Table 1.** List of stratospheric volcanic eruptions used in the study.

673

674 **Table 2.** Summary of tree-ring sites in northeastern Yakutia (YAK), eastern Taimyr (TAY) and  
675 Altai (ALT), and weather stations used in the study. Monthly air temperature (T, °C), precipi-  
676 tation (P, mm), sunshine duration (S, h/month) and vapor pressure deficit (VPD, kPa) data were  
677 used from available meteorological database <http://aisori.meteo.ru/ClimateR>.

678

679

680 **References**

- 681 Abaimov, A.P., Bondarev, A.I., Yzranova, O.V., Shitova, S.A.: Polar forests of Krasnoyarsk  
682 region. Nauka Press, Novosibirsk. 208 p., 1997.
- 683 Battipaglia, G., Cherubini, P., Saurer, M., Siegwolf, R.T.W., Strumia, S., Cotrufo, M.F.: Vol-  
684 canic explosive eruptions of the Vesuvio decrease tree-ring growth but not photosyn-  
685 thetic rates in the surrounding forests. *Global Change Biology*. 13, 1-16, 2007.
- 686 Barinov, V.V., Myglan, V.S., Taynik, A.V., Ojdupaa, O.Ch., Agatova, A.R., Churakova (Si-  
687 dorova) O.V. Extreme climatic events in Altai-Sayan region as indicator of major  
688 volcanic eruptions. *Geophysical processes and biosphere*. 17, 45-61, 2018. doi:  
689 10.21455/GPB2018.3-3.
- 690 Beerling, D.J., Woodward, F.I.: Ecophysiological responses of plants to global environmental  
691 change since the last glacial maximum. *New Phytologist*. 125, 641–648, 1994.
- 692 Boettger T., Haupt, M., Knöller, K., Weise, S., Waterhouse, G.S. ... Schleser, G.H.: Wood  
693 cellulose preparation methods and mass spectrometric analyses of  $\delta^{13}\text{C}$ ,  $\delta^{18}\text{O}$ , and non  
694 ex-changeable  $\delta^2\text{H}$  values in cellulose, sugar, and starch: An inter-laboratory compar-  
695 ison, *Anal. Chem.* 79, 4603–4612, doi:10.1021/ac0700023, 2007.
- 696 Boike, J., Kattenstroth, B., Abramova, K., Bornemann, N., Cherverova, A., Fedorova, I., Fröb,  
697 K., Grigoriev, M., Grüber, M., Kutzbach, L., Langer, M., Minke, M., Muster, S., Piel,  
698 K., Pfeiffer, E.-M., Stoff, G., Westermann, S., Wischnewski, K., Wille, C., Hubberten,  
699 H.-W.: Baseline characteristics of climate, permafrost and land cover from a new per-  
700 mafrost observatory in the Lena Rive Delta, Siberia (1998-2011). *Biogeosciences*. 10,  
701 2105-2128, 2013.
- 702 Briffa, K.R., Jones, P.D., Schweingruber, F.H., Osborn, T.J.: Influence of volcanic eruptions  
703 on Northern Hemisphere summer temperature over the past 600 years. *Nature*. 393,  
704 450–455, 1998.

- 705 Bryukhanova, M.V., Fonti, P., Kirilyanov, A.V., Siegwolf, R., Saurer, M., Pochebyt, N.P., Chu-  
 706 rakova (Sidorova), O.V., Prokushkin, A.S.: The response of  $\delta^{13}\text{C}$ ,  $\delta^{18}\text{O}$  and cell anat-  
 707 omy of *Larix gmelinii* tree rings to differing soil active layer depths. *Dendrochronolo-*  
 708 *gia*. 34, 51-59, 2015.
- 709 Büntgen, U., Myglan, V.S., Ljungqvist, F.C., McCormick, M., Di Cosmo, N., Sigl M., ....Kir-  
 710 dyanov, A.V.: Cooling and societal change during the Late Antique Little Ice Age  
 711 from 536 to around 660 AD. *Nature Geoscience*. 9, 231-236, 2016.
- 712 Cernusak, L., Ubierna, N., Winter, K., Holtum, J.A.M., Marshall, J.D., Farquhar, G.D.: Envi-  
 713 ronmental and physiological determinants of carbon isotope discrimination in terres-  
 714 trial Plants. *Transley Review New Phytologist*. 200, 950-965, 2013.
- 715 Cernusak, L., Barbour, M., Arndt, S., Cheesman, A., English, N., Field, T., Helliker, B., Hol-  
 716 loway-Phillips, M., Holtum, J., Kahmen, A., Mcnerney F, Munksgaard N, Simonin K,  
 717 Song X, Stuart-Williams H, West J and Farquhar G.: Stable isotopes in leaf water of  
 718 terrestrial plants. *Plant, Cell & Environment*. 39 (5), 1087-1102, 2016.
- 719 Churakova (Sidorova), O.V., Bryukhanova, M., Saurer, M., Boettger, T., Naurzbaev, M.,  
 720 Myglan, V.S., Vaganov, E.A., Hughes, M.K., Siegwolf, R.T.W.: A cluster of strato-  
 721 spheric volcanic eruptions in the AD 530s recorded in Siberian tree rings. *Global and*  
 722 *Planetary Change*. 122, 140-150., 2014.
- 723 Churakova (Sidorova), O.V., Shashkin, A.V., Siegwolf, R., Spahni, R., Launois, T., Saurer M.,  
 724 Bryukhanova, M.V., Benkova, A.V., Kupzova, A.V., Vaganov, E.A., Peylin, P., Mas-  
 725 son-Delmotte, V., Roden, J.: Application of eco-physiological models to the climatic  
 726 interpretation of  $\delta^{13}\text{C}$  and  $\delta^{18}\text{O}$  measured in Siberian larch tree-rings. *Dendro-*  
 727 *chronologia*, doi:10.1016/j.dendro.2015.12.008, 2016.

- 728 Cook, E., Briffa, K., Shiyatov, S., Mazepa, V.: Tree-ring standardization and growth trend es-  
729 timation. In: *Methods of dendrochronology: applications in the environmental sci-*  
730 *ences*, Eds: Cook, E.R., Kairiukstis, L.A. 104-123, 1990.
- 731 Cook, E.R., Krusic, P.J.: A Tree-Ring Standardization Program Based on Detrending and Au-  
732 toregressive Time Series Modeling, with Interactive Graphics (ARSTAN). (Ed. by  
733 E.R., Cook and P.J., Krusic), 2008.
- 734 Craig, H.: Isotopic variations in meteoric waters. *Science*. 133, 1702– 1703, 1961.
- 735 Crowley, T.J., Unterman, M.B.: Technical details concerning development of a 1200 yr.  
736 proxy index for global volcanism. *Earth Syst. Sci. Data*. 5, 187-197, 2013.
- 737 Cuny, H.E., Rathgeber, C.B.K., Frank, D., Fonti, P., Fournier, M.: Kinetics of tracheid devel-  
738 opment explain conifer tree-ring structure. *New Phytologist*, 203, 1231–1241, 2014.
- 739 D'Arrigo, R.D., Jacoby, G.C., Frank, D., Pederson, N.D., Cook, E., Buckley, B.M., Nachin, B.,  
740 Mijidorj, R., Dugarjav, C.: 1738-years of Mongolian temperature variability inferred  
741 from a tree-ring width chronology of Siberian pine. *Geophysical Research Letters*.  
742 Vol. 28 (3), 543-546, 2001.
- 743 Dansgaard, W.: Stable isotopes in precipitation. *Tellus*. 16, 436–468, 1964.
- 744 Dawson, T.E., Mambelli, S., Plamboeck, A.H., Templer, P.H., Tu, K.P.: Stable isotopes in plant  
745 ecology *Ann. Review of Ecology and Systematics*. 33, 507-559, 2004.
- 746 Dongmann, G., Förstel, H., Wagener, K.: <sup>18</sup>O-rich oxygen from land photosynthesis. *Nature*  
747 *New Biol.* 240, 127–128, 1972.
- 748 Eschbach, W., Nogler, P., Schär, E., Schweingruber, F.H.: Technical advances in the radioden-  
749 sitometrical determination of wood density. *Dendrochronologia*. 13, 155–168, 2015.
- 750 Esper, J., Büntgen, U., Hartl-Meier, C., Oppenheimer, C., Schneider, L.: Northern Hemisphere  
751 temperature anomalies during 1450s period of ambiguous volcanic forcing. *Bull. Vol-*  
752 *canology*. 79, 41, 2017.

- 753 Farquhar, G. D.: Eds. *Stable Isotopes and Plant Carbon-Water Relations*. Academic Press, San  
754 Diego. 47–70, 1982.
- 755 Farquhar, G.D., Ehleringer, J.R., Hubick, K.T.: *Annu. Rev. Plant Physiol. Plant Mol. Biol.* 40,  
756 503 p, 1989.
- 757 Farquhar, G.D., Lloyd, J.: Carbon and oxygen isotope effects in the exchange of carbon dioxide  
758 between terrestrial plants and the atmosphere. In: Ehleringer, J.R., Hall, A.E., Far-  
759 quhar, G.D. (Eds) *Stable Isotopes and Plant Carbon-Water Relations*. Academic Press,  
760 San Diego, 47–70, 1993.
- 761 Fonti, P., Bryukhanova, M.V., Myglan, V.S., Kirilyanov, A.V., Naumova, O.V., Vaganov,  
762 E.A.: Temperature-induced responses of xylem structure of *Larix sibirica* (Pinaceae)  
763 from Russian Altay. *American Journal of Botany*. 100 (7), 1-12, 2013.
- 764 Francey, R.J., Allison, C.E., Etheridge D.M., Trudinger, C.M., Langenfelds, R.L., Michel, E.,  
765 Steele, L.P.: A 1000-year high precision record of  $\delta^{13}\text{C}$  in atmospheric  $\text{CO}_2$ . *Tellus*.  
766 Ser. B (51), 170-193, 1999.
- 767 Fritts, H.C.: *Tree-rings and climate*. London. New York; San Francisco: Acad. Press. 567 p,  
768 1976.
- 769 Furst, G.G.: *Methods of Anatomical and Histochemical Research of Plant Tissue*. Nauka, Mos-  
770 cow. 156 p, 1979.
- 771 Gao, C., Robock, A., Ammann, C.: Volcanic forcing of climate over the past 1500 years: An  
772 improved ice core-based index for climate models. *J. Geophys. Res. Atmos.*  
773 113:D23111. doi:10.1029/2008jd010239, 2008.
- 774 Gennaretti, F., Huard, D., Naulier, M., Savard, M., Bégin, C., Arseneault, D., Guiot, J.: Bayes-  
775 ian multiproxy temperature reconstruction with black spruce ring widths and stable  
776 isotopes from the northern Quebec taiga. *Clim. Dyn.* doi: 10.1007/s00382-017-3565-  
777 5, 2017.

- 778 Gillett, N.P., Weaver, A.J., Zwiers, F.W. Wehner, M.F.: Detection of volcanic influence on  
779 global precipitation. *Geophysical Research Letters*, 31 (12),  
780 doi:10.1029/2004GL020044 R, 2004.
- 781 Groisman, P.Ya.: Possible regional climate consequences of the Pinatubo eruption. *Geophys.*  
782 *Res. Lett.*, 19, 1603–1606, 1992.
- 783 Gu, L., Baldocchi, D.D., Wofsy, S.C., Munger, J.W., Michalsky, J.J., Urbanski, S.P., Boden,  
784 T.A.: Response of a deciduous forest to the Mount Pinatubo eruption: Enhanced pho-  
785 tosynthesis, *Science*. 299 (5615), 2035–2038, 2003.
- 786 Guillet, S., Corona, C., Stoffel, M., Khodri M., Lavigne F., Ortega, P.,.....Oppenheimer, C.:  
787 Climate response to the 1257 Samalas eruption revealed by proxy records. *Nature ge-*  
788 *oscience*, doi:10.1038/ngeo2875, 2017.
- 789 Hansen, J., Sato, M., Ruedy, R., Lacis, A., Asamoah, K., Borenstein S., ....Wilson, H.: A  
790 Pinatubo climate modeling investigation. In *The Mount Pinatubo Eruption: Effects on*  
791 *the Atmosphere and Climate*, NATO ASI Series Vol. I 42. G. Fiocco, D. Fua, and G.  
792 Visconti, Eds. Springer-Verlag, 233-272, 1996.
- 793 Harrington, C.R.: *The Year without a summer? World climate in 1816*. Ottawa: Canadian  
794 Museum of Nature, ISBN 0660130637, 1992.
- 795 Helama, S., Arppe, L., Uusitalo, J., Holopainen, J., Mäkelä, H.M., Mäkinen, H., Mielikäinen,  
796 K., Nöjd, P., Sutinen, R., Taavitsainen, J.-P., Timonen, M., Oinonen, M.: Volcanic  
797 dust veils from sixth century tree-ring isotopes linked to reduced irradiance, primary  
798 production and human health. *Scientific reports* 8, 1339. doi:10.1038/s41598-018-  
799 19760-w, 2018.
- 800 Hughes, M.K., Vaganov, E.A., Shiyatov, S.G., Touchan, R. & Funkhouser, G.: Twentieth-  
801 century summer warmth in northern Yakutia in a 600-year context. *The Holocene*.  
802 9(5), 603-608, 1999.

- 803 Iles, C.E., Hegerl, G.C.: The global precipitation response to volcanic eruptions in the CMIP5  
804 models. *Environ. Res. Lett.* 9, doi:10.1088/1748-9326/9/10/104012, 2014.
- 805 Joseph, R., Zeng, N.: Seasonally modulated tropical drought induced by volcanic aerosol. *J.*  
806 *Climate*, 24, 2045–2060, 2011.
- 807 Körner, Ch.: Paradigm shift in plant growth control. *Curr. Opinion Plant Biol.* 25, 107-114,  
808 2015.
- 809 Lavigne, F., Degeai, J.-P., Komorowski, J.-C., Guillet, S., Robert, V., Lahitte, P., Oppenhei-  
810 mer, C., Stoffel, M., Vidal, C.M., Suro, I.P., Wassmer, P., Hajdas, I., Hadmoko, D.S.,  
811 Belizal, E.: Source of the great A.D. 1257 mystery eruption unveiled, Samalas vol-  
812 cano, Rinjani Volcanic Complex, Indonesia. *Proc Natl Acad Sci* 110, 16742–16747,  
813 doi:10.1073/pnas.1307520110, 2013.
- 814 Lehmann, M.M., Goldsmith, G.T., Schmid, L., Gessler, A., Saurer, M., Siegwolf, R.T.W.: The  
815 effect of <sup>18</sup>O-labelled water vapour on the oxygen isotope ratio of water and assimilates  
816 in plants at high humidity. *New Phytologist*. 217, 1, 105-116. doi: 10.1111/nph.14788,  
817 2018.
- 818 Lenz, O., Schär, E., Schweingruber F.H.: Methodische Probleme bei der radiographisch-densi-  
819 tometrischen Bestimmung der Dichte und der Jahrrinbreiten von Holz. *Holzforschung*,  
820 30, 114-123, 1976.
- 821 Loader, N.J., Robertson, I., Barker, A.C., Switsur, V.R., Waterhouse, J.S.: Improved technique  
822 for the batch processing of small whole wood samples to alpha-cellulose. *Chemical*  
823 *Geology*. 136, 313-317, 1997.
- 824 Loader, N.J., Young, G.H.F., Grudd, H., McCarroll.: Stable carbon isotopes from Torneträsk,  
825 norther Sweden provide a millennial length reconstruction of summer sunshine and its  
826 relationship to Arctic circulation. *Quaternary Science Reviews*. 62, 97-113, 2013.

- 827 McCarroll, D., Loader, N.J.: Stable isotopes in tree rings. *Quaternary Science Review*. 23, 771-  
828 801, 2004.
- 829 Meronen, H., Henriksson, S.V., Räisänen, P., Laaksonen, A.: Climate effects of northern hem-  
830 isphere volcanic eruptions in an Earth System Model. *Atmospheric Research*, 114-  
831 115: 107-118, 2012.
- 832 Munro, M.A.R., Brown, P.M., Hughes, M.K., Garcia, E.M.R.: Image analysis of tracheid  
833 dimensions for dendrochronological use. *Radiocarbon*, Eds. by M.D. Dean, J.  
834 Swetnam T), pp. 843-851. Tucson, Arizona, 1996.
- 835 Myglan, V.S., Oidupaa, O. Ch., Kirilyanov, A.V., Vaganov, E.A.: 1929-year tree-ring chronol-  
836 ogy for Altai-Sayan region (Western Tuva). *Journal of archeology, ethnography and*  
837 *anthropology of Eurasia*. 4 (36), 25-31, 2008.
- 838 Naurzbaev, M.M., Vaganov, E.A., Sidorova, O.V., Schweingruber, F.H.: Summer temperatures  
839 in eastern Taimyr inferred from a 2427-year late-Holocene tree-ring chronology and  
840 earlier floating series. *The Holocene*. 12(6), 727-736, 2002.
- 841 Panofsky, H.A., Brier, G.W.: *Some applications of statistics to meteorology*. University Park,  
842 PA. Mineral industries extension services, college of mineral industries, Pennsylvania  
843 State University, 1958.
- 844 Panyushkina, I.P., Hughes, M.K., Vaganov, E.A., Munro, M.A.R.: Summer temperature in  
845 northern Yakutia since AD 1642 reconstructed from radial dimensions of larch trache-  
846 ids. *Canadian Journal of Forest Research*. 33, 1-10, 2003.
- 847 Peng, Y., Shen, C., Wang, W.-C., Xu, Y.: Response of summer precipitation over Eastern China  
848 to large volcanic eruptions. *Journal of Climate*. 23, 818-824, 2009.
- 849 R Core Team.: *R: A Language and Environment for Statistical Computing*. Vienna, Austria,  
850 2016.
- 851 Robock, A.: Volcanic eruptions and climate. *Reviews of Geophysics*. 38(2), 191-219, 2000.



- 852 Robock, A., Liu, Y.: The volcanic signal in Goddard Institute for Space Studies three-dimensional model simulations. *J. Climate*. 7, 44-55, 1994.
- 853
- 854 Roden, J.S., Siegwolf, R.: Is the dual isotope conceptual model fully operational? *Tree Physiology*. 32, 1179-1182, 2012.
- 855
- 856 Saurer, M., Kirilyanov, A.V., Prokushkin, A.S., Rinne K.T., Siegwolf, R.T.W.: The impact of an inverse climate–isotope relationship in soil water on the oxygen-isotope composition of *Larix gmelinii* in Siberia. *New Phytologist*. 109, 3, 955-964, 2016.
- 857
- 858
- 859 Saurer, M., Robertson, I., Siegwolf, R., Leuenberger, M.: Oxygen isotope analysis of cellulose: an interlaboratory comparison. *Analytical chemistry*, 70, 2074-2080, 1998.
- 860
- 861 Saurer, M., Kirilyanov, A. V., Prokushkin, A. S., Rinne, K. T., Siegwolf, R.T.W.: The impact of an inverse climate-isotope relationship in soil water on the oxygen-isotope composition of *Larix gmelinii* in Siberia. *New Phytologist*. 209(3), 955-964, 2016.
- 862
- 863
- 864 Scheidegger, Y., Saurer, M., Bahn, M., Siegwolf, R.: Linking stable oxygen and carbon isotopes with stomatal conductance and photosynthetic capacity: a conceptual model. *Oecologia*. 125, 350–357. DOI: 10.1007/s004420000466, 2000.
- 865
- 866
- 867 Schneider, L., Smerdon, J.E., Büntgen, U., Wilson, R.J.S., Myglan, V.S., Kirilyanov, A.V., Esper, J.: Revising mid-latitude summer temperatures back to A.D. 600 based on a wood density network. *Geophys. Res. Lett.* 42, GL063956, Doi:10.1002/2015gl063956, 2015.
- 868
- 869
- 870
- 871 Schweingruber, F.H.: *Tree rings and environment dendroecology*. Paul Haupt Publ Bern, Stuttgart, Vienna 1996. pp. 609, 1996.
- 872
- 873 Sidorova, O.V., Naurzbaev, M.M.: Response of *Larix cajanderi* to climatic changes at the upper timberline and in the Indigirka River valley. *Lesovedenie (in Russian)*. 2, 73-75, 2002.
- 874

- 875 Sidorova, O.V.: Long-term climatic changes and the larch radial growth on the northern Middle  
876 Siberia and the Northeastern Yakutia in the Late Holocene. Abs. PHD Diss, V.N.  
877 Sukachev Institute of Forest, Krasnoyarsk, 2003.
- 878 Sidorova, O.V., Naurzbaev, M.M., Vaganov, E.A.: Response of tree-ring chronologies growing  
879 on the Northern Eurasia to powerful volcanic eruptions. Problems of ecological moni-  
880 toring and ecosystem modeling, XX, 60-72, 2005.
- 881 Sidorova, O.V., Saurer, M., Myglan, V.S., Eichler, A., Schwikowski, M., Kirilyanov, A.V.,  
882 Bryukhanova, M.V., Gerasimova, O.V., Kalugin, I., Daryin, A., Siegwolf, R.: A  
883 multi-proxy approach for revealing recent climatic changes in the Russian Altai. Cli-  
884 mate Dynamics, 38 (1-2), 175–188, 2011.
- 885 Sidorova, O.V., Siegwolf, R., Myglan, V.S., Loader, N.J., Helle, G., Saurer, M.: The applica-  
886 tion of tree-rings and stable isotopes for reconstructions of climate conditions in the  
887 Altai-Sayan Mountain region. Climatic Changes, doi: 10.1007/s10584-013-0805-5,  
888 2012.
- 889 Sidorova, O.V., Siegwolf, R., Saurer, M., Naurzbaev, M., Shashkin, A.V., Vaganov, E.A.: Spa-  
890 tial patterns of climatic changes in the Eurasian north reflected in Siberian larch tree-  
891 ring parameters and stable isotopes. Global Change Biology, doi: 10.1111/j.1365-  
892 2486.2009.02008.x, 16, 1003-1018, 2010.
- 893 Sidorova, O.V., Siegwolf, R.T.W., Saurer, M., Naurzbaev, M.M., Vaganov, E.A.: Isotopic  
894 composition ( $\delta^{13}\text{C}$ ,  $\delta^{18}\text{O}$ ) in Siberian tree-ring chronology. Geophysical research  
895 Biogeosciences. 113, 1-13, 2008.
- 896 Sigl, M., Winstrup, M., McConnell, J.R.: Timing and climate forcing of volcanic eruptions for  
897 the past 2500 years. Nature. 523, 543-549. doi:10.1038/nature14565, 2015.

- 898 Sprenger, M., Tetzlaff, D., Buttle, J. M., Laudon, H., Leister, H., Mitchell, C., Snelgrove, J.,  
899 Weiler, M., Soulsby, C.: Measuring and modelling stable isotopes of mobile and bulk  
900 soil water, *Vadose Zone Journal*, <https://doi.org/10.2136/vzj2017.08.0149>, 20, 2017.
- 901 Sternberg, L.S.O.: Oxygen stable isotope ratios of tree-ring cellulose: The next phase of un-  
902 derstanding. *New Phytologist*. 181 (3), 553-562, 2009.
- 903 Stirzaker, D.: *Elementary Probability density functions*. Cambridge. Sec. Ed. 538 p, 2003.
- 904 Stoffel, M., Khodri, M., Corona, C., Guillet, S., Poulain, V., Bekki, S., Guiot, J., Luckman,  
905 B.H., Oppenheimer, C., Lebas, N., Beniston, M., Masson-Delmotte, V.: Estimates of  
906 volcanic-induced cooling in the Northern Hemisphere over the past 1,500 years. *Nature*  
907 *Geoscience*. 8, 784–788, 2015.
- 908 Stothers, R.B.: Climatic and Demographic Consequences of the Massive Volcanic Eruption of  
909 1258. *Climatic Change*. 45, 361-374, 2000.
- 910 Stothers, R.B.: Mystery cloud of AD 536. *Nature*. 307, 344-345, doi:10.1038/307344a0, 1984.
- 911 Sugimoto, A., Yanagisawa, N., Fujita, N., Maximov, T.C.: Importance of permafrost as a  
912 source of water for plants in east Siberian taiga. *Ecological Research*. 17 (4), 493-  
913 503, 2002.
- 914 Toohey, M., Sigl, M.: Volcanic stratospheric sulphur injections and aerosol optical depth  
915 from 500 BCE to 1900 CE. *Earth System Science Data*. doi:10.5194/essd-9-809-  
916 2017, 2017.
- 917 Vargas, A. I., Schaffer, B., Yuhong, L. Sternberg, L.S.: Testing plant use of mobile vs immo-  
918 bile soil water sources using stable isotope experiments. *New Phytologist*. 215, 582–  
919 594, doi: 10.1111/nph.14616, 2017.
- 920 Vaganov, E.A., Hughes, M.K., Kirilyanov, A.K., Schweingruber, F.H., Silkin, P.P.: Influence  
921 of snowfall and melt timing on tree growth in subarctic Eurasia. *Nature*. 400, 149-151,  
922 1999.

- 923 Vaganov, E.A., Hughes, M.K., Shashkin, A.V.: Growth dynamics of conifer tree rings. Springer  
924 Verlag, Berlin., pp. 353, 2006.
- 925 Wegmann, M., Brönnimann, S., Bhend, J., Franke, J., Folini, D., Wild, M., Luterbacher, J.:  
926 Volcanic influence on European summer precipitation through monsoons: Possible  
927 cause for “years without summer”. AMS, doi.org/10.1175/JCLI-D-13-00524.1, 2014.
- 928 Wigley, T.M.L., Briffa, K.R., Jones, P.D.: On the Average Value of Correlated Time Series,  
929 with Applications in Dendroclimatology and Hydrometeorology. *Journal of Climate*  
930 and Applied Meteorology. 23 (2), 201-213, doi:10.1175/15200450(1984)023.0201,  
931 1984.
- 932 Wiles, G.C., D’Arrigo, R.D., Barclay, D., Wilson, R.S., Jarvis, S.K., Vargo, L., Frank, D.: Sur-  
933 face air temperature variability reconstructed with tree rings for the Gulf of Alaska  
934 over the past 1200 years. *The Holocene*. 6, 2014. 10.1177/0959683613516815.
- 935 Wilson, R.J.S., Anchukaitis, K., Briffa, K. et al.: Last millennium Northern Hemisphere sum-  
936 mer temperatures from tree rings. Part I: the long-term context. *Quaternary Science*  
937 *Review*. 134, 1–18, 2016.
- 938 Zielinski, G.A., Mayewski, P.A., Meeker, L.D., Whitlow, S., Twickler, M.S., Morrison, M.,  
939 Meese, D.A., Gow A.J., Alley, R.B.: Record of volcanism since 7000 BC from the  
940 GISP2 Greenland ice core implications for the volcano-climate system. *Science*. 264  
941 (5161), 948-952, 1994.